Mem. Fac. Eng., Osaka City Univ., Vol. 45, pp. 29 – 36 (2004)

A Study on Reinforced Concrete Columns Under Cyclic Biaxial Moment

Tomoaki SATO,[1] Harutoshi KOBAYASHI,[2] and Hisao TSUNOKAKE[3]

(*Received September 30, 2004*)

Synopsis

Reinforced concrete columns for the bridge pier model are subjected to the combined cyclic and constant loads in the main and sub horizontal directions, respectively, and also the constant vertical axial load. Test parameters for five loading cases are the intensity factor of the constant load in the sub horizontal direction which varies as 0, 25, 50 and 75 % of its horizontal yield load. All five specimens failed in a flexural mode. The peak strength of the cyclic load decreased as the constant load increased. The interaction relation due to biaxial loadings obtained is discussed. In the numerical analysis, the simple stress-strain relation models for the confined concrete and reinforcement according to the Japanese seismic design cord were used. Good agreements about the maximum load are obtained, but the numerical load values in the unloading state are larger than experimental ones.

Key Words: *biaxial horizontal loads, cyclic loading, experiment, interaction curve, method of fiber model, numerical analysis, RC column model*

1. Introduction

A large number of investigations on the loading capacity of reinforced concrete (RC) columns for bridge pier model under uniaxial horizontal loads have been already performed experimentally and/or numerically. However, well knowledge on the mechanical behavior and loading capacity of the RC columns under biaxial moments are required for the seismic resistant structure design, because actual seismic ground motions are essentially three-dimensional. Therefore, some studies on the RC column models under biaxial moments have been made experimentally and/or numerically, for examples, by Chen and Shoraka [1], Yoshimura et al. [2], Kuroda [3], Hayakawa et al. [4], etc.

This paper firstly examines experimentally the mechanical behavior of the RC column models under the combined cyclic and constant loads in the main and sub horizontal directions, respectively. Five identical tenth scaled specimens were tested. The test parameter was the intensity of the constant horizontal load that varied as 0, 25, 50 and 75 % of its horizontal yield load. In addition, the constant vertical axial load related to the self-weight of the superstructures whose magnitude was almost 15 % of axial yield load was also applied. Hysteresis loops of load-displacement relation, interaction curves on cyclic and constant loads and failure modes obtained from the biaxial loading tests are discussed.

To assess the experimental results, secondly, numerical analyses were made by using the partitioning method (method of fiber model) for the RC cross section [1, 2] and the simple stress-strain relation models for the confined concrete and reinforcement according to the Japanese seismic design cord [5]. Maximum load values and hysteresis loops of load-displacement relation are examined.

2. Cyclic Biaxial Horizontal Loading Tests

2.1. Test specimen

Figure 1 shows the front and cross-sectional views of test specimen with its reinforcement. The specimen was a tenth scaled model of a practical bridge pier with a square cross section of 2.5 m in side length, which was designed to fail in not shear mode but flexural mode according to the Japanese seismic design

[1]Doctor Course Student (JIP Techno Science Corporation), Division of Civil Engineering, Department of Urban Engineering
[2]Professor, Division of Civil Engineering, Department of Urban Engineering
[3]Research Associate, Division of Civil Engineering, Department of Urban Engineering

cord [5]. Deformed steel bars of 13 mm in nominal diameter and round steel bars of 6 mm in diameter were used as the longitudinal reinforcement and hoop tie, respectively.

Table 1 presents the material properties measured at the day when each test was carried out. Table 2 indicates the horizontal load intensity and horizontal displacement related to flexural crack occurrence in concrete, initial yielding of longitudinal reinforcement and ultimate state due to a flexural failure estimated by the Japanese seismic design cord [5].

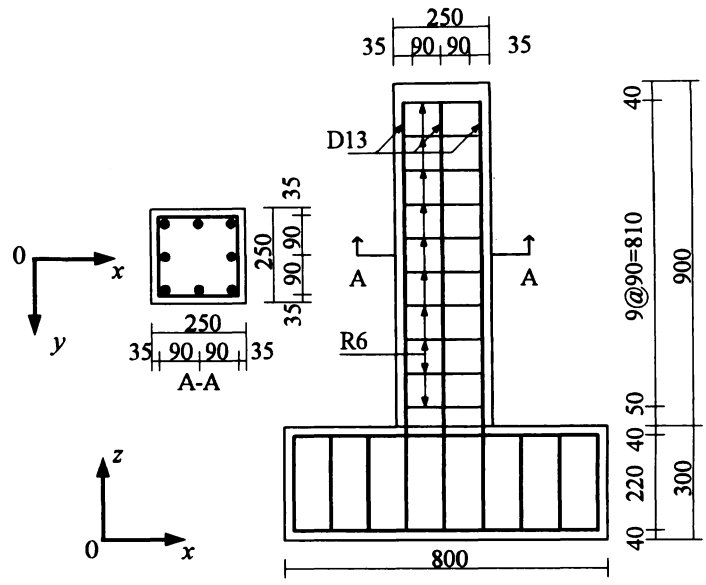

Fig. 1 Experimental member details (unit : mm)

Table 1 Material properties

Materials (N/mm^2)		Specimen No.			
		1	2	3	4
Concrete	Compressive strength f_c	30.2	30.2	28.8	31.5
	Young's modulus E_c ($\times 10^4$)	2.65	2.65	2.86	2.98
Longitudinal reinforcement	Yield strength f_y	378	378	378	378
	Ultimate strength f_u	522	522	522	522
	Young's modulus E_s ($\times 10^5$)	1.75	1.75	1.75	1.75
Hoop tie	Yield strength f_y	239	239	239	239
	Young's modulus E_s ($\times 10^5$)	1.71	1.71	1.71	1.71

Table 2 Displacement and strength for uniaxial bending

State	Displacement (mm)		Strength (kN)	
Flexural crack occurrence in concrete	δ_c	0.190	P_c	11.241
Yield of longitudinal reinforcement	$\delta_{x,yield}$	2.208	$P_{x,yield}$	52.342
Ulitimate of longitudinal reinforcement	δ_u	9.364	P_u	55.252

2.2. Loading program

The directions of biaxial horizontal loading used in this study are shown in Fig. 2, in which $x-$ and $y-$ axes indicate the main and sub directions for the cyclic load F_x and the constant load F_y, respectively, and u and v are the displacements. The constant load F_y is defined by

$$F_y = \alpha P_{x,yield} \tag{1}$$

where $P_{x,yield}$ is the initial yield strength corresponding to yielding of longitudinal reinforcement at a certain section of the RC column due to the uniaxial horizontal loading, and α is the load intensity factor that shall be taken as 0, 2.5, 0.5 and 0.75 for each specimen as presented in Table 3. The specimen 1 ($\alpha = 0$),

therefore, was tested under the cyclic uniaxial loading. Loads were applied at the points whose distance from the RC column foot was taken as 800 mm. During testing, all the specimens were also subjected to the constant vertical axial load related to the self-weight of the superstructures upon the pier, whose magnitude was almost 15 % of the axial yield load.

The cyclic loading program in the $x-$direction (main direction) followed the displacement-controlled condition as illustrated in Fig. 3, in which $\mu = u/\delta_{x,yield}$ is the displacement factor and $\delta_{x,yield}$ is the yield horizontal displacement corresponding to the initial yield strength $P_{x,yield}$ and these values are given in Table 2. Each specimen was subjected to the cyclic loading of one cycle to displacement factors of each of $\mu = \pm 0.5,\ \pm 1,\ \pm 1.5,\ \pm 2,\ \ldots$ up to $\mu = 5$, and then after this state until failure, subsequent loading performed under the conditions of displacement factors of $\mu = \pm 6,\ \pm 7,\ \pm 8, \ldots$.

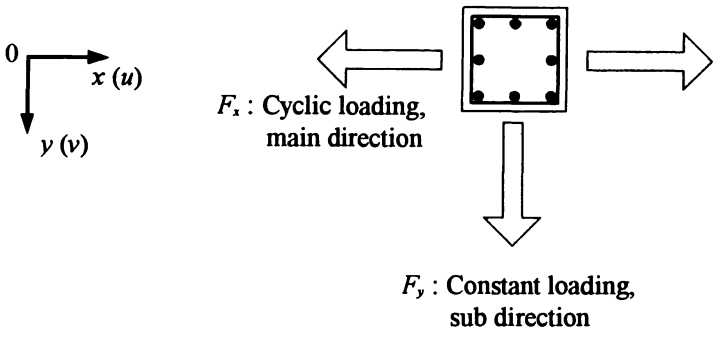

Fig. 2 Loading directions

Table 3 Loading program

Specimen No.	1	2	3	4
x-direction, F_x	Cyclic	Cyclic	Cyclic	Cyclic
y-direction, F_y	Constant $\alpha = 0$	Constant $\alpha = 0.25$	Constant $\alpha = 0.50$	Constant $\alpha = 0.75$
Parameter α is applied to Eq.(1).				

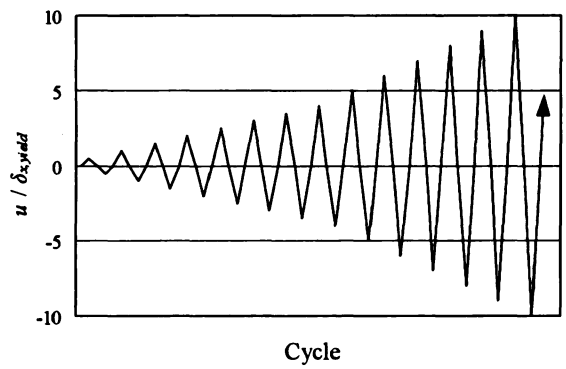

Fig. 3 Cyclic loading program in x-direction under displacement-controlled condition

2.3. Test results

Figure 4 presents the hysteresis loops of relation of the cyclic horizontal load F_x and displacement u for the cases of $\alpha = 0.25$, 0.5 and 0.75. For the purpose of comparison the hysteresis loop for the case of cyclic uniaxial loading ($\alpha = 0$) is also depicted in the same figures. The marked points A and B indicate, respectively, the maximum load points for the case of $\alpha = 0$ and each other case of α. The maximum value of the cyclic load F_x decreases as the load intensity factor α increases, i.e. their values are 52.5, 51.3, 46.9 and 42.8 kN for the cases of $\alpha = 0$, 0.25, 0.5 and 0.75, respectively.

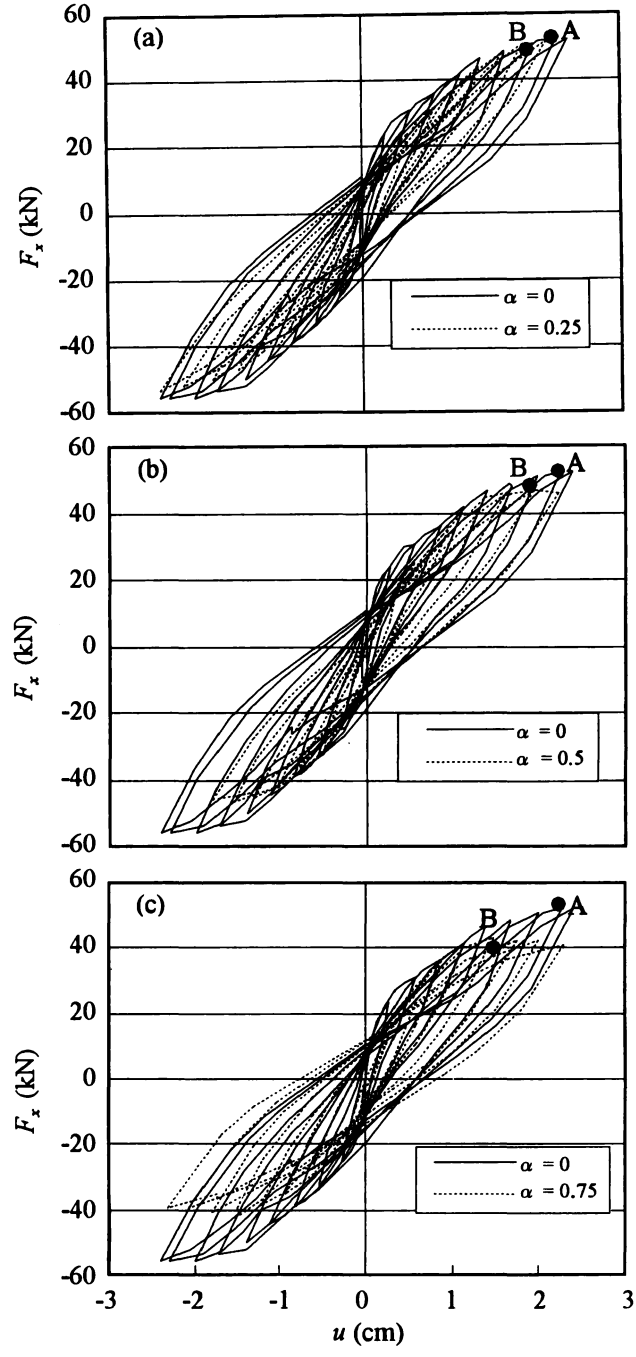

Fig. 4 Hysteresis loops of F_x and u relation

The relation of the maximum values of cyclic load F_x and constant load F_y obtained by the tests for all the cases of α are plotted in Fig. 5, in which the interaction curve of F_x and F_y are also depicted by using the following interaction equation [6]:

$$\left(\frac{F_x}{F_{x,yield}}\right)^{\beta} + \left(\frac{F_y}{F_{x,yield}}\right)^{\beta} = 1 \tag{2}$$

where $F_{x,yield}$ means the yield load of the uniaxial loading case ($\alpha = 0$) and may be evaluated by using the partitioning method (method of fiber model) [1, 2] in conjunction with the stress-strain relation models for the concrete and reinforcement considering the confinement effect and strain hardening effect, respectively [5]. Details of numerical procedure are given in the next section. It is found from the figure that the

interaction curves with the exponent $\beta = 2$ and 3 may well approximate the test results.

Figure 6 shows the failure mode of specimen 3 ($\alpha = 0.5$). From this figure, the compressive failure modes are seen on the side Y_B and at both the corners A and B, and the flexural cracks are also observed around the column surfaces.

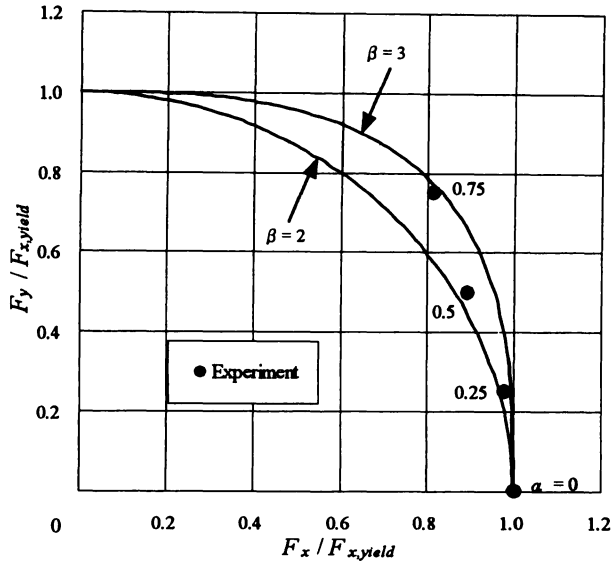

Fig. 5 Test results and interaction curves of F_x and F_y given by Eq. (2)

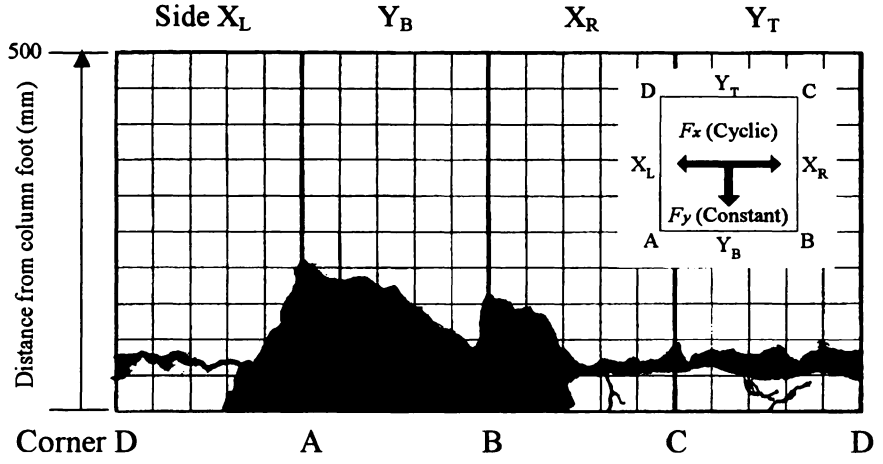

Fig. 6 Failure mode of specimen 3 ($\alpha = 0.5$)

3. Numerical Study

3.1. Numerical procedure

To assess numerically the test results mentioned in the previous section, the partitioning method (method of fiber model) for the RC column cross section [1, 2] is employed. The assumption of this method is as follows:

(1) The strain distribution across the cross section varies proportionally to the distance from the neutral axis, i.e. plane cross sections remain plane during the bending.

(2) The stresses are treated to be constant in divided each element, and thus the strain and stress in each element are computed as the average value at its centroid.

Figure 7 shows the stress-strain relation model for the concrete that is considered with the confinement effect by the hoop tie according to the Japanese seismic design code [5]. In this figure, the following

notations are used: σ_c is the stress of concrete; σ_{cc} (=31.2 N/mm^2) the compressive strength of the confined concrete; σ_{bt} (=2.2 N/mm^2) the tensile strength of concrete; ε_c the strain of concrete; ε_{cc} (=0.00256) the strain of concrete at the peak stress; ε_{cu} (=0.00334) the ultimate strain of the confined concrete; E_c Young's modulus of concrete; and E_{des} (=8,000 N/mm^2) the descending gradient after the peak stress.

In this study, the decrease inclination line has been extended from the point of ultimate stress (strain) to the point of intersection of inclination line with the strain axis, and it is assumed for the unloading and reloading processes that the stress-strain relation follows the inclination of initial Young's modulus E_c. Therefore, the envelope curves of stress-strain relation of the confined concrete are given by the following expressions:

$$\sigma_c = E_c\varepsilon_c\left[1-\frac{1}{n}\left(\frac{\varepsilon_c}{\varepsilon_{cc}}\right)^{n-1}\right] \quad \text{when} \quad 0 \le \varepsilon_c \le \varepsilon_{cc} \tag{3a}$$

$$\sigma_c = \sigma_{cc} - E_{des}(\varepsilon_c - \varepsilon_{cc}) \quad \text{when} \quad \varepsilon_{cc} \le \varepsilon_c \tag{3b}$$

where n is defined by

$$n = \frac{E_c\varepsilon_{cc}}{E_c\varepsilon_{cc} - \sigma_{cc}} \tag{4}$$

On the other hand, the skeleton curves of the stress-strain relation of the reinforcement are shown in Fig. 8 by the solid line. It is treated as the bi-liner model considering the strain hardening effect. These skeleton curves are expressed by the following equations:

$$\sigma_s = E_s\varepsilon_s \quad \text{when} \quad \varepsilon_s \le |\varepsilon_{sy}| \tag{5a}$$

$$\sigma_s = E_s'(\varepsilon_s - \varepsilon_{sy}) + \sigma_{sy} \quad \text{when} \quad \varepsilon_s > \varepsilon_{sy} \tag{5b}$$

$$\sigma_s = E_s'(\varepsilon_s + \varepsilon_{sy}) - \sigma_{sy} \quad \text{when} \quad \varepsilon_s < -\varepsilon_{sy} \tag{5c}$$

where σ_s is the stress of reinforcement; σ_{sy} (=378 N/mm^2) the yield strength of reinforcement; ε_s the strain of reinforcement; ε_{sy} (=0.0216) the yield strain of reinforcement; E_s Young's modulus of reinforcement;

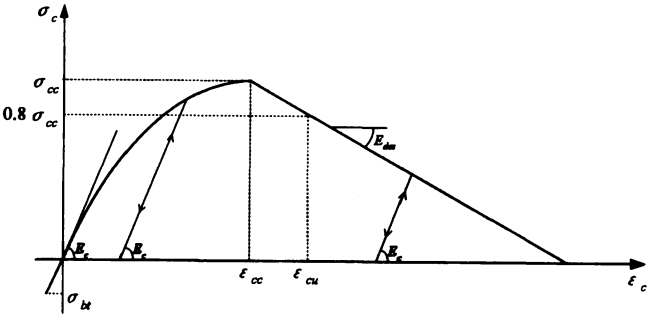

Fig. 7 Stress-strain relation for concrete

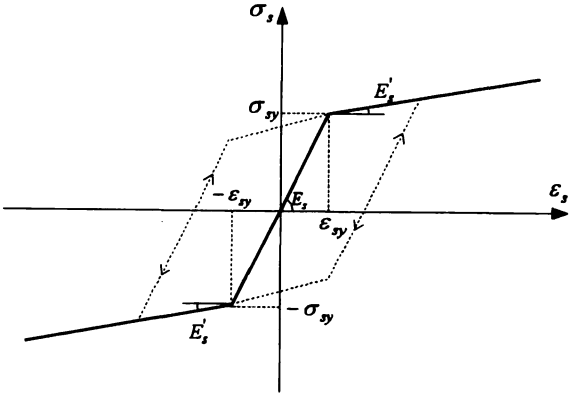

Fig. 8 Stress-strain relation for reinforcement

and E_s' ($=0.0095E_s$) Young's modulus of reinforcement at strain hardening process.

For the unloading and reloading processes expressed by the dotted line, it is assumed that the stress-strain relation follows the inclination of initial Young's modulus E_s as well as the case of concrete.

3.2. Numerical results

Figure 9 (a) displays the comparison between the experimental and numerical results for the case of a monotonous loading of F_x ($F_y = 0$) whose experimental results have not been presented in the previous section 2. On the other hand, Fig. 9 (b) shows the comparison results for the case of simultaneously applied two equal loads F_x and F_y ($= F_x$) to the $x-$ and $y-$ directions, respectively. This figure depicts three relations, i.e. the load F_x and displacement u relation, the load F_y and displacement v relation, and the resultant load of magnitude $(F_x^2 + F_y^2)^{1/2}$ and resultant displacement of magnitude $(u^2 + v^2)^{1/2}$ relation. In both the figures, the solid and dotted lines indicate numerical and experimental results, respectively. Numerical results are obtained as the monotonous loading case. It can be found from two figures that the numerical results show almost good agreements with the experimental ones.

Next, the numerical analyses for the biaxial bending for three cases of $\alpha = 0.25$, 0.5 and 0.75 were carried out under the displacement-controlled condition. Here, only the relation of load F_x and displacement u for the case of $\alpha = 0.5$ (specimen 3) is presented in Fig. 10. The solid and dotted lines indicate numerical and experimental results, respectively. Although both the maximum load values from

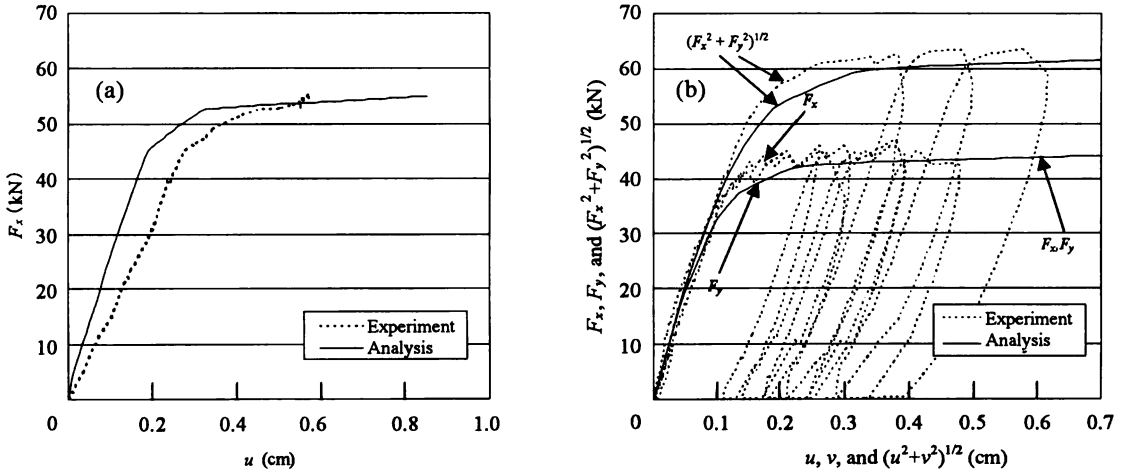

Fig. 9 Experimental and numerical results for : (a) uniaxial bending by F_x and (b) biaxial bending by F_x and F_y ($=F_x$)

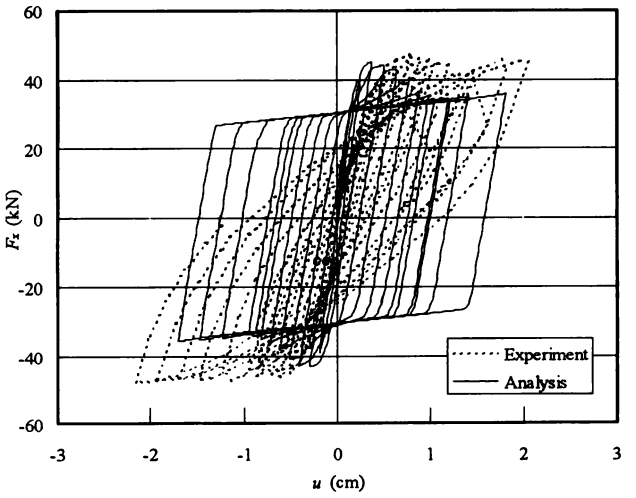

Fig. 10 Comparison of hiysteresis loops of F_x and u relation of specimen 3 ($\alpha = 0.5$)

experimental and numerical results show good agreement, the differences are seen about the decrease of each loop after the maximum load value. Moreover, at the unloading processes, the experimental load values are large than the numerical one. Similar results are also obtained for other two cases.

4. Concluding Remarks

The flexural strength of RC columns for bridge pier model subjected to the combined cyclic and constant horizontal loads in the main and sub directions and the constant vertical axial load has been investigated experimentally and numerically.

Five identical tenth scaled specimens were tested. The test parameter was taken as the load intensity factor α for the constant horizontal load that varied as 0, 25, 50 and 75 % of its horizontal yield load. Following main results are obtained: (1) The maximum load decreases as the load intensity factor α increases; (2) The interaction relation of F_x and F_y with the factor $\beta = 2$ and 3 may well approximate the test results; and (3) The compressive failure modes are observed on the side of the sub direction.

Subsequent numerical analyses using the partitioning method (method of fiber model) and the simple stress-strain relations for concrete and reinforcement show that the maximum load can be estimated with good accuracy, but differences between the experimental and numerical results are seen after the maximum load or during the unloading process.

References

[1] Chen, W. F. and Shoraka, M. T.: Tangent stiffness method for biaxial bending of reinforced concrete columns, *IABSE Publications*, International Association for Bridge and Structural Engineering, Vol. 35/I, pp. 23-44, 1975

[2] Yoshimura, M., Aoyama, H., and Kawamura, M.: Analysis of reinforced concrete structure subjected to two-dimensional forces, Part 1: Analysis of RC columns subjected to bi-axial bending. *Journal of Structural and Construction Engineering (Transactions of AIJ)*, Architectural Institute of Japan, No. 298, pp. 31-41, 1980 (in Japanese)

[3] Kuroda, Y.: A study on three directional deformation characteristics of reinforced concrete columns, Master Thesis, Department of Architecture and Building Engineering, Tokyo Metropolitan University, March 1995 (in Japanese)

[4] Hayakawa, R., Kawashima, K., and Watanabe, G: Effect of bilateral loadings on the flexural strength and ductility of reinforced concrete bridge columns, *Proceedings of Japan Society of Civil Engineers (JSCE)*, No.759/I-67, pp. 79-98, April 2004 (in Japanese)

[5] Japan Road Association: *Specifications for Highway Bridges*; *Part V- Seismic Design*, Maruzen, Tokyo, 2002 (in Japanese)

[6] Bresler, B.: Design criteria for reinforced concrete columns under axial load and biaxial bending, *Journal of the American Concrete Institute (ACI)*, Vol. 57, No. 5, pp. 481-490, November 1960